Noninvasive Testing Methods: Multifocal Electrophysiology

E E Sutter, The Smith - Kettlewell Eye Research Institute, San Francisco, CA, USA

Glossary

Base interval of stimulation – Stimuli are presented at intervals that are integral multiples of a base interval.
Binary stimulation – The stimulation that switches between two states such as flash/no flash, pattern–contrast-reversing pattern.
First-order kernel – This response component is computed by adding the response signal following base intervals with a stimulus and subtracting the signal following intervals without stimulus. If the response is linear, response contributions from subsequent stimuli must cancel as they are added and subtracted the same number of times. If the response is nonlinear, the following responses depend on the presence of the preceding stimulus. The difference that appears in the first-order kernel is called an induced component.
Inion – The prominent projection of the occipital bone at the lower rear part of the skull.
Lamina cribrosa – A mesh-like structure through which the optic nerve exits the sclera.
M-sequence stimulation – The binary stimulation controlled by a special class of pseudorandom binary sequences called m-sequences. These sequences have ideal properties for the analysis of nonlinear systems.
Myelination – An electrically insulating material that forms a layer, surrounding the axons of many neurons. Axons of retinal ganglion cells become myelinated at the lamina cribrosa in the optic nerve head. Myelination of axons greatly increases the propagation velocity of action potentials.
Nonlinear response – In the case of binary stimulation, nonlinear means that the contribution of a response to the signal may depend on preceding and immediately following responses or responses in the neighboring areas.
Saltatory nerve conduction – The nerve conduction in myelinated fibers whereby the action potential jumps from gap to gap between the myelinated section.
Second-order, first slice – This response component can roughly be thought of as the difference between the response to two consecutive stimuli and the two stimuli individually presented.

Why Multifocal?

Visual electrophysiology has enjoyed decades of useful applications in the clinic and research. It provides objective measures of function at different stages of visual processing. Until relatively recently, it has been restricted to testing of a single area in the visual field. In the clinic it was generally used as a full field test or a test of a single area or spot in the field. This has greatly limited its sensitivity in diagnosis and in measuring progression and recovery from disease. It was clear from the start that mapping responses across the retina recording focal responses from one small area at a time would have taken very long and would not be practical. Multifocal techniques have overcome this limitation by stimulating a large number of areas concurrently whereby the response of each area is encoded in its temporal stimulation pattern. The special encoding using binary m-sequences permits clean extraction of the focal response contributions from a single signal derived from the cornea or from the scalp over the visual cortex of the brain. The m-sequence encoding has the additional benefit that it provides information on nonlinear response properties such as fast adaptation and recovery from photo stress that can be important clinical indicators.

There are many multifocal protocols available to clinicians. Some of them test the central visual field with lower spatial resolution and short recording times useful for screening. Others offer high resolution for the detection of small scotomata and sensitive assessment of changes in the spatial extent of dysfunction. Yet, other protocols enhance inner retinal and specifically ganglion-cell contributions. These tools permit tailoring the test for a specific clinical purpose. In many laboratories, only one protocol is commonly used and ordered by the clinicians as a multifocal electroretinogram (mfERG). Judicious selection of one of many available tests can lead to faster and more accurate diagnosis and, in some cases, avoid errors. Careful data analysis by a knowledgeable user can tease out local-response abnormalities that might otherwise be missed. A few examples shown below are selected to illustrate this point.

The Basic Principle

The basic principle of mfERG and multifocal visual-evoked potential (mfVEP) recording is schematically illustrated in **Figure 1**. With both types of recordings, the size of the focal stimuli is scaled with eccentricity to

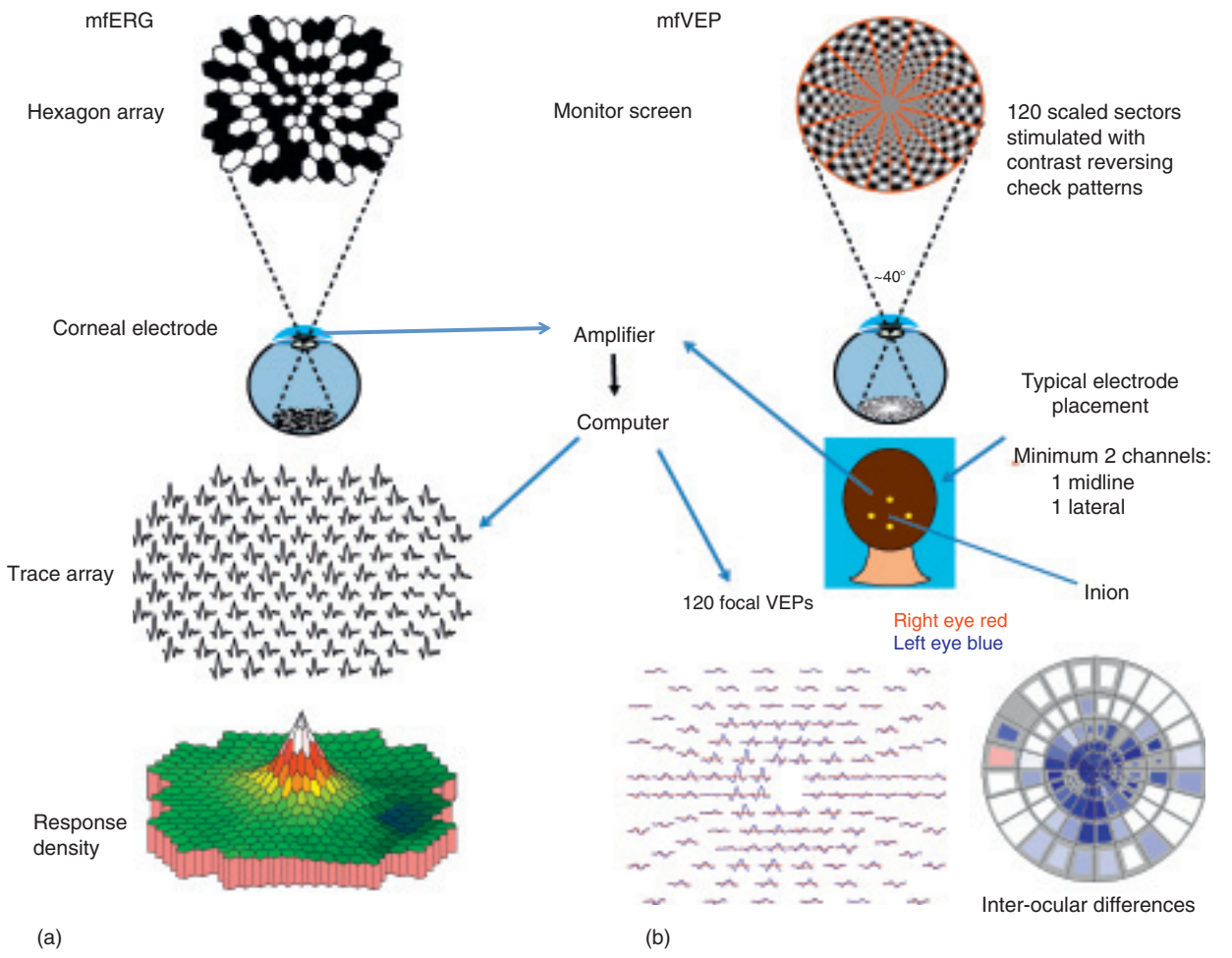

Figure 1 Schematic representation of the derivation of mfERG and mfVEP records. Commonly used stimulus arrays are shown on top. For the mfERG, hexagonal arrays are scaled with eccentricity to achieve similar signal-to-noise ratios across the stimulated field. The focal stimulation is m-sequence modulated flicker. The corneal signal can be derived with any of the available electrode techniques. For mfVEP, recording a dartboard pattern of stimulus elements is used to account for the steep eccentricity scaling of the representation of the visual field on the primary visual cortex. Each sector is stimulated with a contrast-reversing check pattern. Two perpendicular electrode pairs pasted to the scalp over the primary visual cortex cover the different directions of current flow. The data are presented as an expanded array of traces (bottom left) and as a pseudocolor field map (bottom right). The example is from an asymmetric patient. The left eye largely dominates (blue areas) except in the area of the right-eye blind spot (pink patch).

generate approximately the same signal amplitudes across the stimulated field. In the mfERG, we use scaled hexagonal arrays of the kind shown in **Figure 1(a)**. The steeper scaling of the cortical response requires the use of dartboard patterns **Figure 1(b)**. While the mfERG stimulus is usually focal flicker, the cortical responses of the multifocal visual-evoked cortical potential (mfVECP) are best elicited with focal contrast reversal of a check pattern.

Recording of Multifocal Data

All the data presented here have been recorded, analyzed, plotted, and exported with VERIS science 6.0 (Electro-Diagnostic Imaging, Inc, Redwood City, CA, USA). The mfERG data were recorded with a Burian–Allen bipolar contact lens electrode. This electrode and others of similar construction provide the best signal-to-noise ratio. Disposable monopolar electrodes such as the DTL fiber or the HK loop are considered less invasive but provide noisier signals and require longer recording times to achieve the same-quality data. Contact lens electrodes offer the advantage that they correct for corneal astigmatism and prevent drooping eyelids. However, care must be taken that the corneal ring of the electrode is reasonably well centered on the dilated pupil. To be comfortable, the electrode should be selected to fit the size of the eye.

All mfERG records shown here were recorded with a stimulus screen calibrated to produce multifocal flash intensities of 2.7 cd s m^{-2}. In most cases, the patient's fixation stability was monitored with an eye camera. For more recent recordings, fixation was monitored with an

infrared (IR) fundus camera that shows the position of the stimulus array on the fundus of the eye throughout the recording.

Multifocal Stimulators

Originally monochrome cathode ray tubes (CRTs) with a fast white phosphor were commonly used for stimulation. Few color CRTs could reach the required stimulus intensity. While, at this time, some suitable CRT monitors are still available, this technology is rapidly disappearing from the market and is being replaced by flat-panel liquid crystal display (LCD) monitors. The large panels are now bright enough, but achieve high brightness by leaving the pixels on during the entire display frame. This is ideal for pattern-reversal stimulation such as the mfVEPs, but it is not recommended for mfERGs. The switching speed of these panels is also marginal for ERG recording but adequate for mfVEPs. For multifocal flash ERG recording, we would like to have brief focal flash stimuli of no more than 2–3-ms duration at the beginning of each frame. This can be achieved with some of the available microdisplays. DLP projection displays can be used after substantial internal modifications.

Patient Positioning and Data Collection

In many laboratories chin rests are used for stabilization of the patient's head during recording. This is acceptable, but not the best solution. Patients are more comfortable in a reclining chair with a stable adjustable headrest. The reclined position helps to keep contact lens electrodes from dropping out. This arrangement works well in combination with a small stimulator mounted on an articulating arm. It allows adjustment of the angle of the stimulator so that the corneal ring of the contact lens electrode is centered on the patient's pupil.

The stimulus normally consists of a single cycle of a binary m-sequence. Using a longer m-sequence rather than averaging several shorter ones prevents contamination by higher-order kernels and, thus, provides cleaner separation of the local response contributions. For patient comfort, the record is collected in slightly overlapping segments that permit smooth splicing before data processing. Protocols for contact lens electrodes use a segment size of about 30 s. When recording with fiber electrodes, the patient must suppress blinks. To make this easier for the patient, the segment size is reduced to about 15 s.

Data Analysis and Presentation

Focal responses are extracted from the recorded signal using a cross-correlation executed by the fast m-transform. The focal responses may be contaminated with noise from blinks and small eye movements. A special artifact subtraction algorithm helps clean up the data. If the quality is not sufficient for this purpose, the operator can apply spatial filtering whereby each local waveform is averaged with a certain percentage of its nearest neighbors. This greatly improves the waveforms, but leads to some local smearing and is not recommended in cases where dysfunctional areas are suspected to be very small.

Clinically useful parameters of the local response waveforms can be extracted and presented as pseudo-color 2- or 3-dimensional topographic maps. The two most important ones are maps of response density and peak implicit time (time from the stimulus onset to the selected peak). Response densities are derived by dividing each focal-response amplitude by the solid visual angle of the corresponding stimulus patch. Estimating amplitudes of the often noisy focal responses using peak-to-trough measurements is very inaccurate. For this reason, a method of template matching is used. Each focal waveform is multiplied point by point with a normalized template of the underlying response. The template is derived as the average of waveforms in the same retinal region.

Implicit times of specific features of the response waveform, that is, the time from the stimulus onset to the feature are sensitive clinical measures. Of particular importance is the implicit time of the main positive peak *P*1. Estimating *P*1 implicit times using the highest point in the waveform is much too inaccurate when dealing with the noisy local responses. Much more accurate estimates are achieved by means of a template of the underlying waveform. On each focal waveform, the template is shifted into the position of best mean square fit. The location of the peak on the template waveform is then taken as the implicit time estimate. As with the amplitude estimation described above, the template waveform used at each location is the average of waveforms in the same neighborhood.

Dealing with Noisy Data

The main contaminations in mfERG responses are artifacts from blinks and small eye movements. It is possible to detect these artifacts and subtract them from the recorded signal. The process is capable of recovering some of the responses superimposed on the artifact, as long the artifact did not saturate data acquisition. This noise-reduction procedure works very well with mfERG records, but is less effective with mfVEPs where the contamination is usually noise from muscle tone required to maintain head posture rather than discrete artifacts. Here, it is more important to position the head in order to minimize tension.

How Long Does the Test Take?

The kernel extraction is an averaging procedure and, thus, follows the law of averages. Increasing the recording time

by a factor k improves the signal-to-noise ratio by $k^{1/2}$. The duration of a test must be determined by the amount of information to be gained and the signal-to-noise ratio of the derived response.

A multitude of tests can be designed from very short tests to tests lasting perhaps 1 h or more. The longer tests are used when more precise information is required. In the selection of a test, one should consider all the information already known regarding the patient.

Figure 2(**a**) and **2**(**b**) show the results from two very short recordings derived from the same subject. Sixty-one patches stimulated the central field. Interpolating hexagons were inserted at plotting time to permit a more accurate estimation of the topography. The signal quality was very good in this case and does not reflect what one might get from an average patient in such ultra-short recording times. However, recordings of 2-min duration can be quite adequate for patient screening.

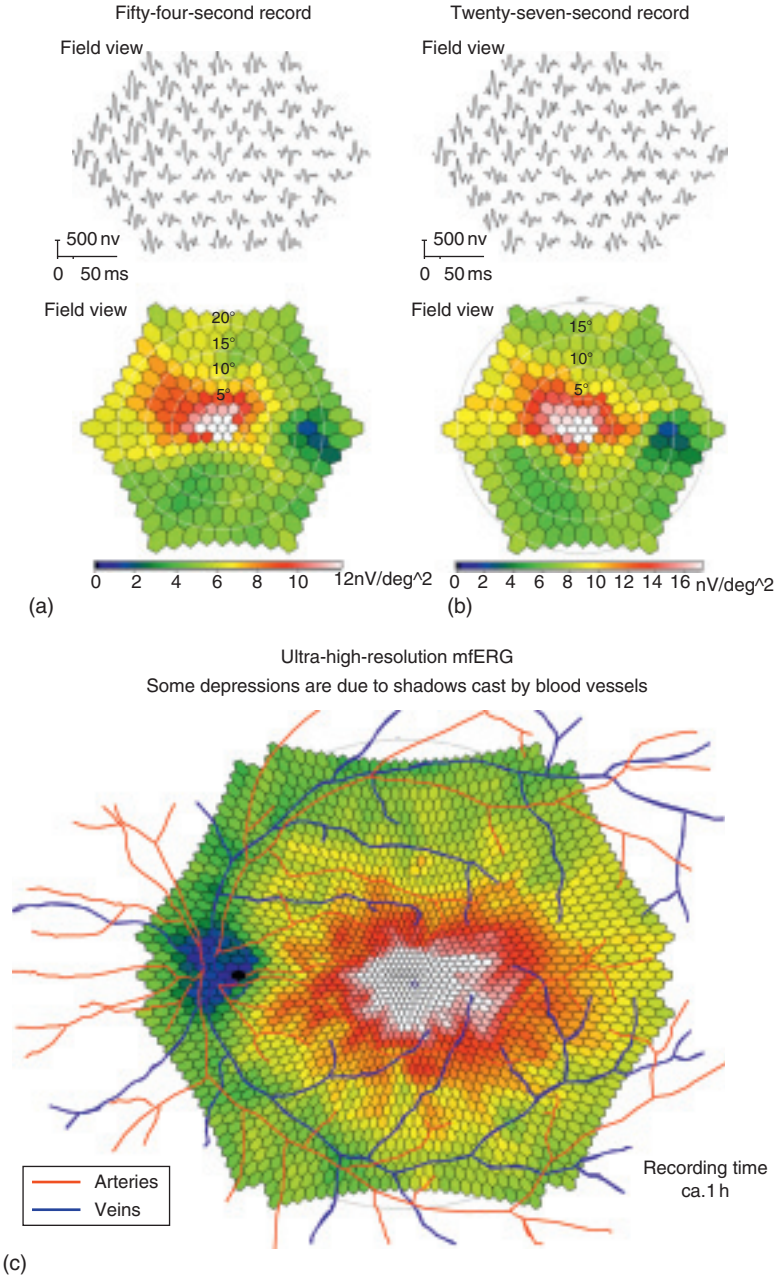

Figure 2 (a) Results from two very short multifocal recordings with 61 stimulus areas. The signals were derived with a bipolar Burian–Allen electrode. (b) High resolution recording using 509 stimulus areas within the central 45° of the visual field. The overlaid vasculature of the subject suggests that the depressed responses in some areas are caused by shadows of major blood vessels and their bifurcations.

Figure 2(**c**) illustrates a high-resolution recording with a stimulus array of 509 patches. The recording time of about 1 h necessary for this resolution is clearly not feasible in the clinic. The most popular array size uses 103 hexagons and records of 2–7 min length. Some clinics have used 241 hexagons in 7-min tests. Ideally, the spatial resolution of the test should be adjusted to meet the requirements of the clinical problem at hand.

Some Examples from the Retina Clinic

The samples presented below are selected to illustrate uses of different recording and analysis protocols. The clinical significance of the results cannot be discussed here due to space limitations.

Central Serous Retinopathy

The first example is from a male patient with central serous retinopathy (CSR). He was not diagnosed at the time of the recording but complained about a relative central scotoma in his left eye. We selected a 7-min test with 241 hexagonal patches because of the anticipated small spatial extent of the problem. The plots shown represent the average of two records. Individual records are slightly noisier, but would have been quite adequate in this case. **Figure 3**(**a**) shows the response density plots of the two eyes. The affected area in the left eye is clearly visible as an excavation in the central peak extending to the area surrounding the optic nerve head. The right eye is normal.

Some pathologies cause local delays in the main positive peak of the first-order waveform called the *P*1 peak indicated by the marks on the traces in **Figure 3**(**c**). Such delays are mainly attributed to photoreceptor sensitivity loss. Mapping the peak implicit time can help distinguish between different pathologies. In this CSR case, such delays are found in areas with reduced response density (**Figure 3**(**b**)).

Plots of *P*1 implicit time generally show delays in the vicinity of the disk. This feature must be ignored. It is attributed to a contribution to the focal response from scattered light. Some light from the focal stimulation of the highly reflective optic disk is scattered onto the peripheral retina where it elicits a delayed response contribution.

Hydroxychloroquine Retinopathy

A small percentage of patients who take this drug for autoimmune disease develop a bull's eye retinopathy. This dysfunction is, at best, only partially reversible when the patient is taken off the drug. For disease prevention, the mfERG is now proposed as a test for patient screening.

The left column in **Figure 4**(**a**) shows a typical example of hydrohychloroquine toxicity. Only the right eye is shown here as the presentation is usually bilaterally symmetric. The array of traces is shown at the top followed by the plots of response density and *P*1 implicit time below. Responses surrounding the center are substantially reduced to about 7–10° eccentricity with some relative sparing of the center.

The bottom plots shows that hydroxychloroquine toxicity does not cause significant changes in peak implicit times. This suggests that the changes are post-receptoral.

Amplitude ratios of ring averages around the fovea are used for diagnosis and assessment of severity of the bull's eye presentation. A plot from an automated screening protocol with statistical evaluation is shown in **Figure 5**. Ring averages are plotted in **Figure 5**(**a**). In **Figure 5**(**b**), response densities are plotted against eccentricity in degrees of visual angle and compared to data from a normal cohort. The data are interpolated with a cubic spline. For this analysis, ring averages have been normalized to the outermost ring that is usually minimally affected. The green bands around the normal mean (red line) represent the 2 standard deviation (SD) limit. The heavy black line is the patient's response amplitude. The area where the patient curve falls outside the 2-SD band is colored red. ICS is the index of central sparing used to evaluate the bull's eye configuration. It is computed as the ratio between the red area outside 3° eccentricity and the total red area below the 2-SD band. An ICS number of 1 indicates that all the losses in amplitude relative to the peripheral ring are outside 3° with complete sparing of the center. In a typical maculopathy patient, we find ICS values of around 0.2–0.4.

The importance of considering implicit times as well as response densities in standard clinical testing is illustrated with the example shown in the right-hand column of **Figure 4** showing a patient with unknown vision loss.

The patient's visual fields showed a bilateral bull's eye configuration reminiscent of hydroxychloroquine toxicity of **Figure 4**(**a**). The perifoaveal relative scotoma seen in the visual field is confirmed by the response density distribution of the mfERG (**Figure 4**(**a**)). However, in this case we see substantial delays in the areas with depressed response amplitudes. This finding suggests loss in receptor sensitivity. In this case, topographic mapping of *P*1 implicit times was needed to clearly distinguish this case from hydroxychloroquine toxicity. Latency plots are often necessary to distinguish different pathologies with similar response density topography.

Juvenile X-Linked Retinoschisis

The first-order trace array (**Figure 6**(**a**)) and the first-order response density plots (**Figure 6**(**b**)) show two areas where amplitudes are still within normal range. However, closer scrutiny reveals that the two areas are very different in their functional properties. Area 1 is normal in the

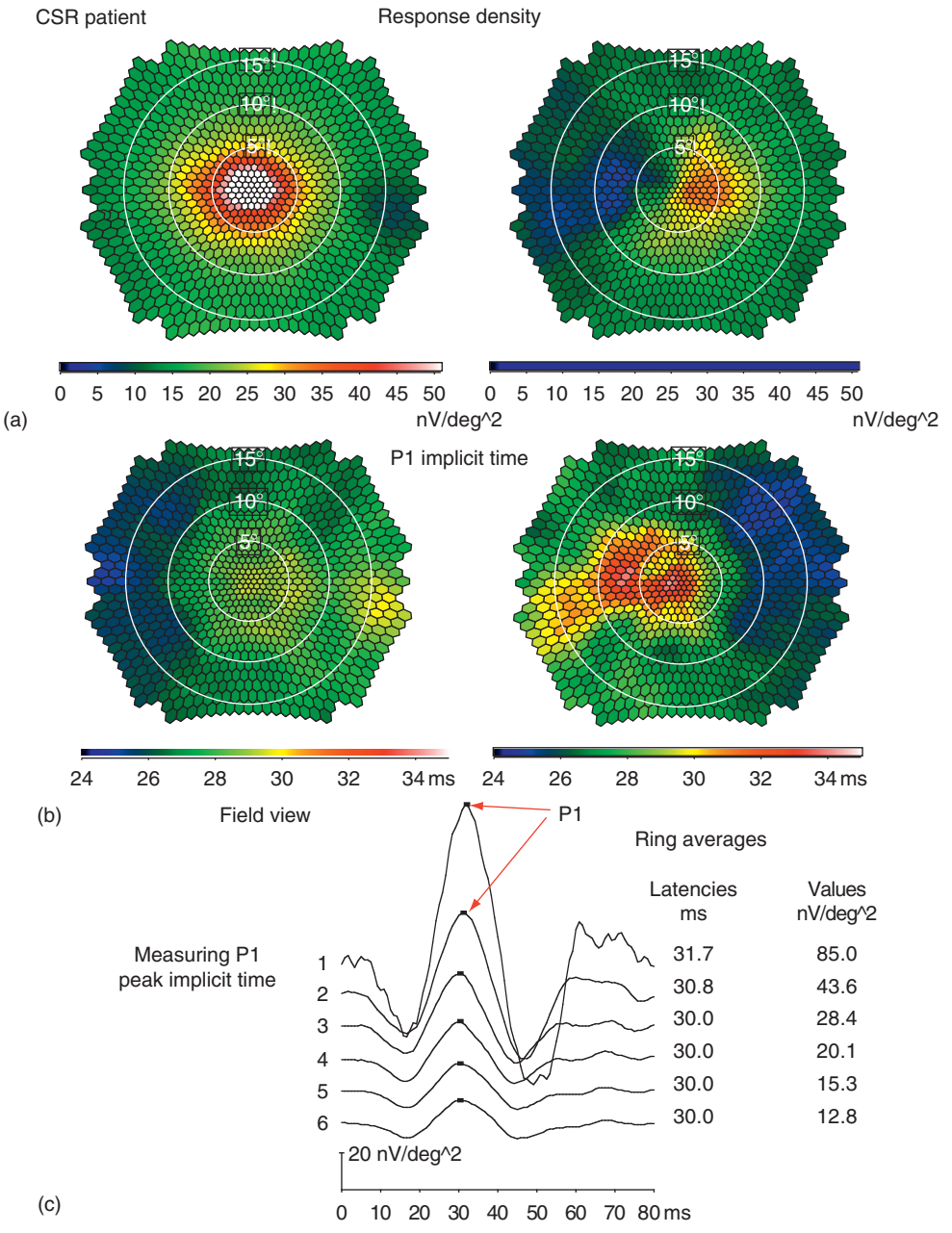

Figure 3 A patient complaining of a relative central scotoma diagnosed as central serous retinopathy with the help of this test. (a) A response density plot derived from two 7-min records. (b) The plot of *P*1 implicit time from the same record. *P*1 implicit times are measured from the time of the focal flash to the first positive peak as shown in (c).

first-order response amplitude as well as the *P*1 implicit time. The dominant higher-order component, the first slice of the second-order kernel, is also within normal range. This component reflects interactions between consecutive flash responses and is thought to originate predominantly in the inner retina. Area 2, on the other hand, has highly abnormal implicit times of close to 40 ms. The second-order component is almost completely absent in this area. This case illustrates the importance of looking not only at response densities but also at peak implicit times and the dominant higher-order kernel.

Detecting Small Central Dysfunction

The patient complained of a very small scotoma. It did not show in the visual field (**Figure 7(b)**) and there was no abnormal ophthalmoscopic finding. The patient drew the scotoma in the Amsler grid at 5° eccentricity (**Figure 7(a)**). Due to the small size of the suspected central dysfunction, we selected a protocol that places all 103 hexagons within the central 12°. The net recording time was 7 min. A distinct depression is seen at the location corresponding to the Amsler grid drawing (**Figure 7(a)**). In such cases, no spatial

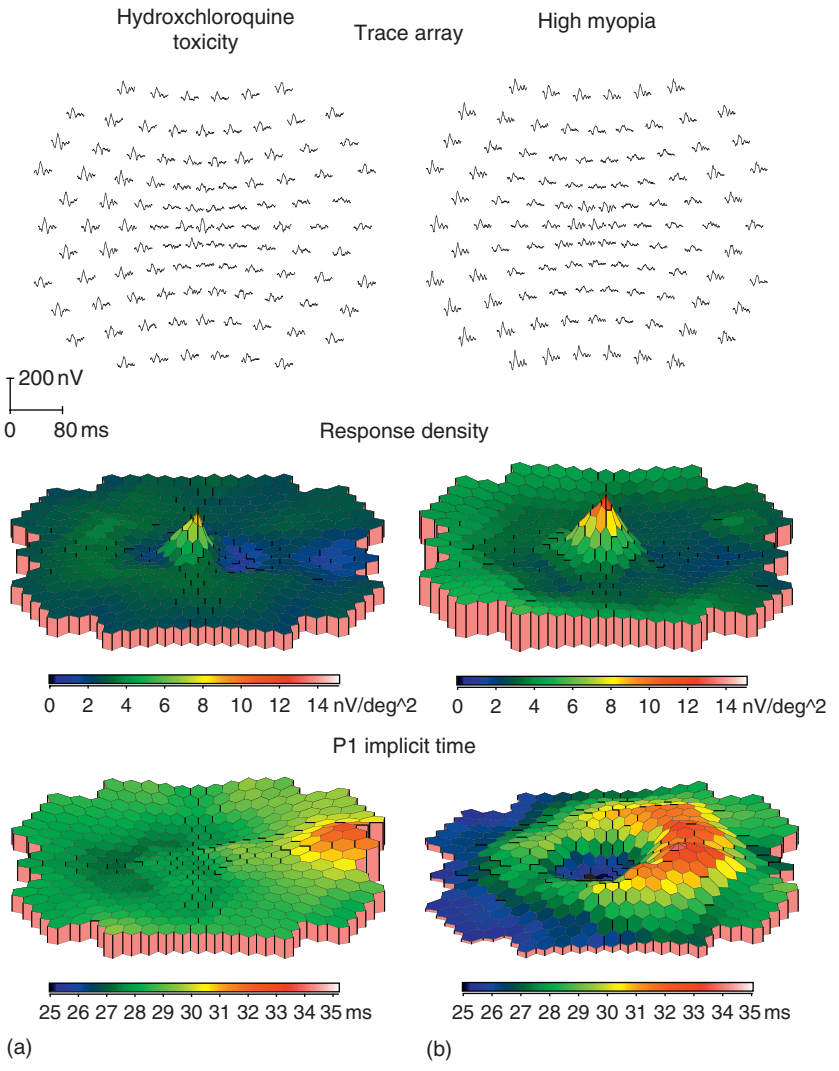

Figure 4 Column (a) shows a typical case of hydroxychloroquine toxicity. The characteristic peri-central amplitude loss is clearly seen in the trace array and the response density plot. The plot of *P*1 implicit time is normal suggesting inner retinal abnormalities. The enhancement in the area of the optic disc is due to scattered light and can be ignored. (b) a patient (high myopia) with a peri-central scotoma resembling hydroxychloroquine retinopathy. The increased implicit times in the depressed areas suggests a different pathogenesis, namely photoreceptor sensitivity loss. Plots of implicit time were needed to distinguish the two pathologies.

filtering could be applied to improve the quality of the focal waveforms as this would greatly reduce the small depression seen in the plot.

Another application of high-resolution central recording of this type is follow-up to macular hole surgery. OCT records document repair of structure, while the mf ERG can be used to map recovery of function over time.

Applications to Neuro-Ophthalmology and Glaucoma

Some of the most important future clinical applications of multifocal electrophysiology are expected in the area of neuro-ophthalmology and glaucoma. The integrity of the optic pathway can be tested using the visual-evoked cortical response derived by means of electrodes placed over the visual cortex as schematically illustrated on the right in **Figure 1**. The response to contrast reversal of a check pattern has been shown to be most sensitive for the detection of conduction losses to the cortex. The introduction of the multifocal pattern visual-evoked response (mfVEP) raised hopes for objective visual field mapping. The main obstacle to this aim is found in the convoluted cortical anatomy onto which the visual field is mapped. Different patches in the visual field generate dipole signal sources of different orientations. Adequate coverage of the visual field requires at least two electrode pairs at perpendicular orientation as well as their sum and difference signals. Uniform coverage is not possible. Comparison

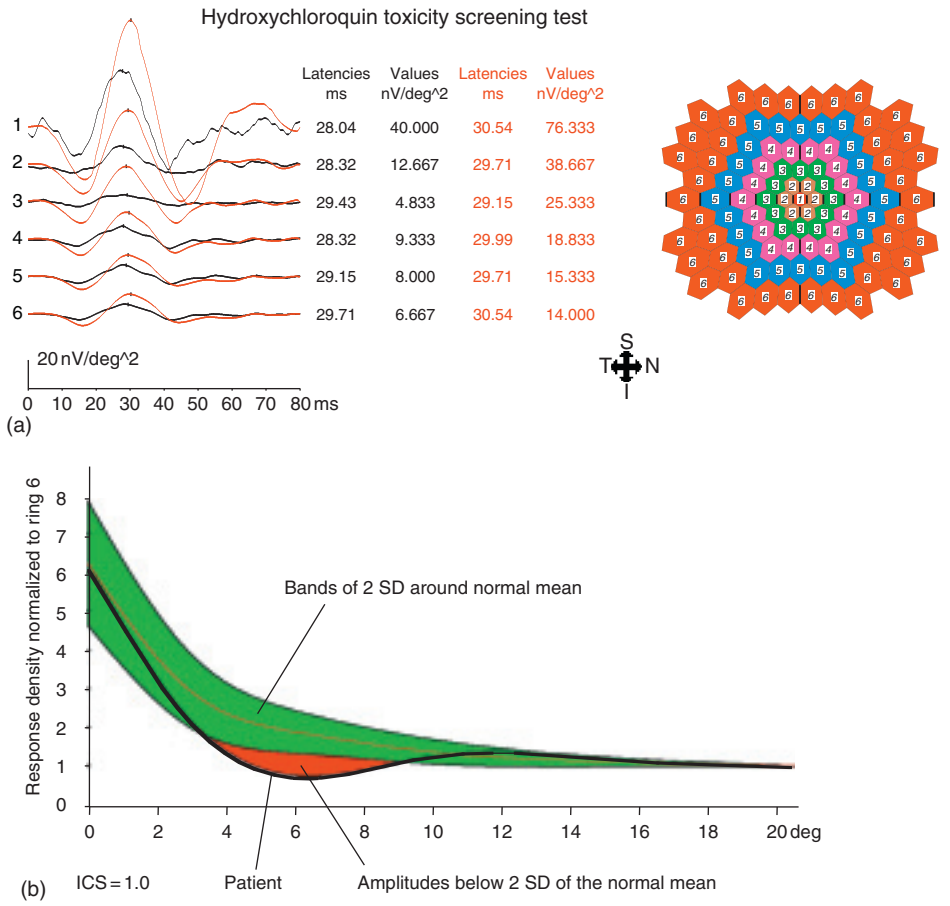

Figure 5 Automated statistical analysis for hydroxychloroquine toxicity screening. (a) responses in six rings for the patient (black) and the mean of 46 normal eyes (red). In (b), the amplitudes are plotted as a function of eccentricity. All data have been normalized to the outermost ring that is relatively unaffected in this condition. The ring averages of 5(a) are plotted as a function of eccentricity in degrees of visual angle with cubic spline interpolation. The green bands indicate 2-SD around the normal mean. The patient plot is in black.

with normative data is problematic due to the intersubject differences in the gross cortical anatomy. However, interocular comparison makes the mfVECP a powerful tool when the pathology is monocular or asymmetric between the eyes. Stimuli at corresponding locations in the visual field of the two eyes project to the same cortical patch and, in normal subjects, elicit virtually identical responses.

The cortical fold at the bottom of the calcarine fissure presents a problem that cannot be addressed with multiple electrodes. Sectors of the stimulus whose projections fall in this cortical area may wrap around the fold such that the same stimulus patch stimulates opposing surfaces of the sulcus generating mutually canceling dipole sources. This leads to characteristic signal dropout in the vicinity of the horizontal meridian. A substantial improvement was achieved by subdividing the sectors further and recording with 120 rather than 60 sectors. To compensate for resulting loss in signal to noise, the signal of each sector is averaged with a given percentage of the surrounding sectors after they have been brought to the same signal polarity. A typical plot of a trace array from a normal subject is shown in **Figure 8(a)**. Traces from the right eye are red, left eye traces blue. In this presentation, the position of the traces is not topographic. They are approximately equally spaced to best utilize the rectangular plot surface. The approximate eccentricities of the waveforms are indicated with black contour lines. The plot was derived from two perpendicular electrode placements, one from electrodes on the midline 4 cm apart and the other from electrodes 4 cm lateral to the inion on both sides. At each stimulus location, the signal-to-noise ratios of the two recorded channels and their sum and difference signals were compared and the best combination was selected. The pseudo-color topographic map of **Figure 8(b)** was derived from the same record. It graphically represents the local differences in response amplitude between the two eyes. The saturation of the color in each stimulus patch indicates the interocular difference while the amount of gray in each patch is a measure of uncertainty. It is derived from the noise level in the record. While some data can also be displayed in numeric form, this graphic representation permits us to capture

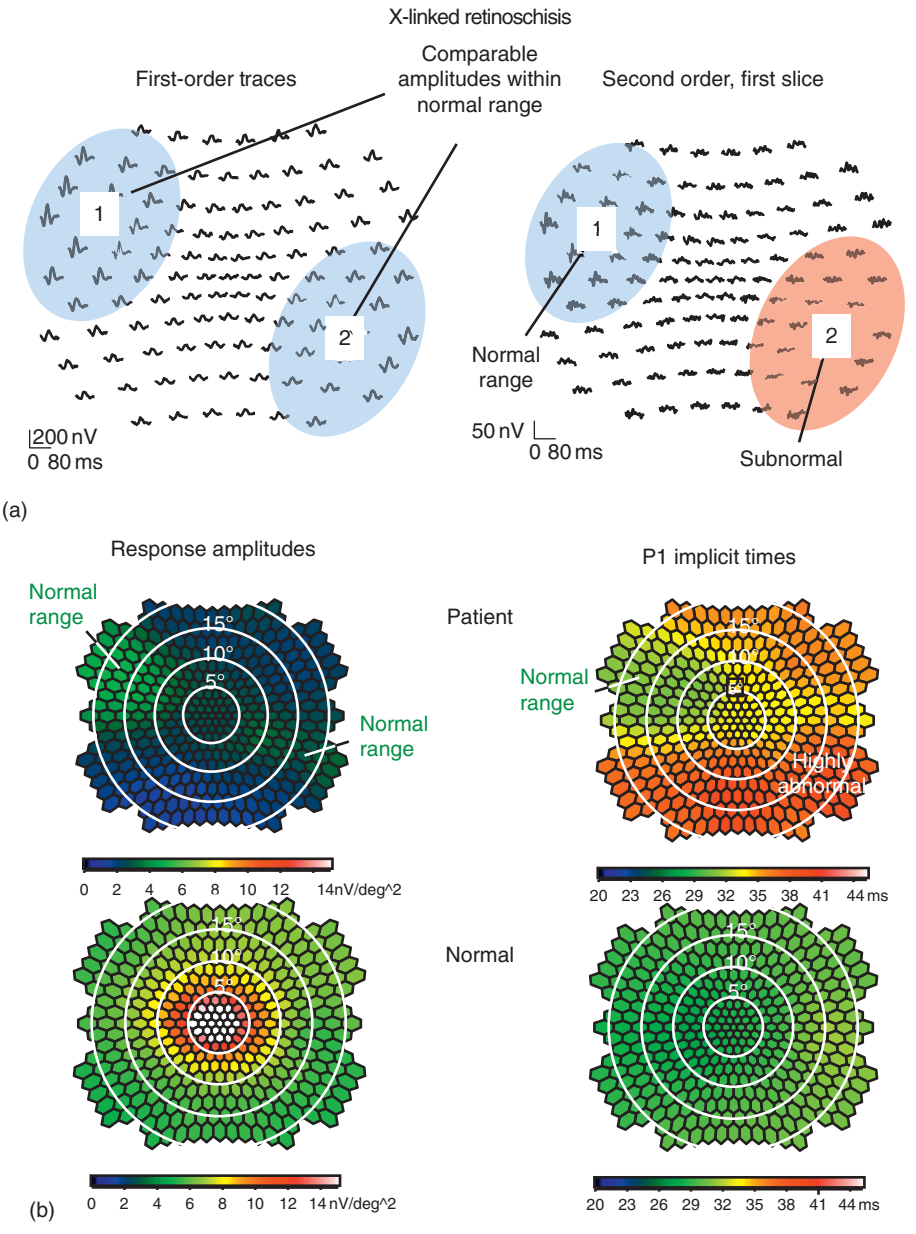

Figure 6 Record from right eye of a patient with x-linked juvenile retinoschisis. (a) The first-order traces show two areas with amplitudes within normal range. However, in area 2, the dominant second-order response contributions are almost completely extinct. (b) The response density plot shows two islands of relatively normal amplitudes. While the *P*1 implicit times are normal in area 1, they are highly abnormal in area 2.

the essence at a glance. Note that even in normal subjects, areas with small interocular differences in the peripheral areas are not unusual.

The mfVECP in Optic Neuritis

An obvious application of the mf VECP is in optic neuritis and multiple sclerosis. It is illustrated here with an example of acute optic neuritis. **Figure 9** shows mf VECP plots recorded in the acute phase and at 2-month intervals during recovery. In the acute phase, the responses within the central 3° of the affected eye are almost extinguished. The first follow-up record shows substantial recovery of amplitudes in this area, while increased implicit times indicate areas of demyelination. In the second follow-up record, the implicit times in the lower part of the fovea are back to normal, while in the upper field the delays persist.

Comparison of the mfVEP and the mf ERG in Optic Neuropathies and Glaucoma

It is well known that the ERG signal contains contributions from retinal ganglion cells and that losses of this cell population can, through a retrograde process, affect other

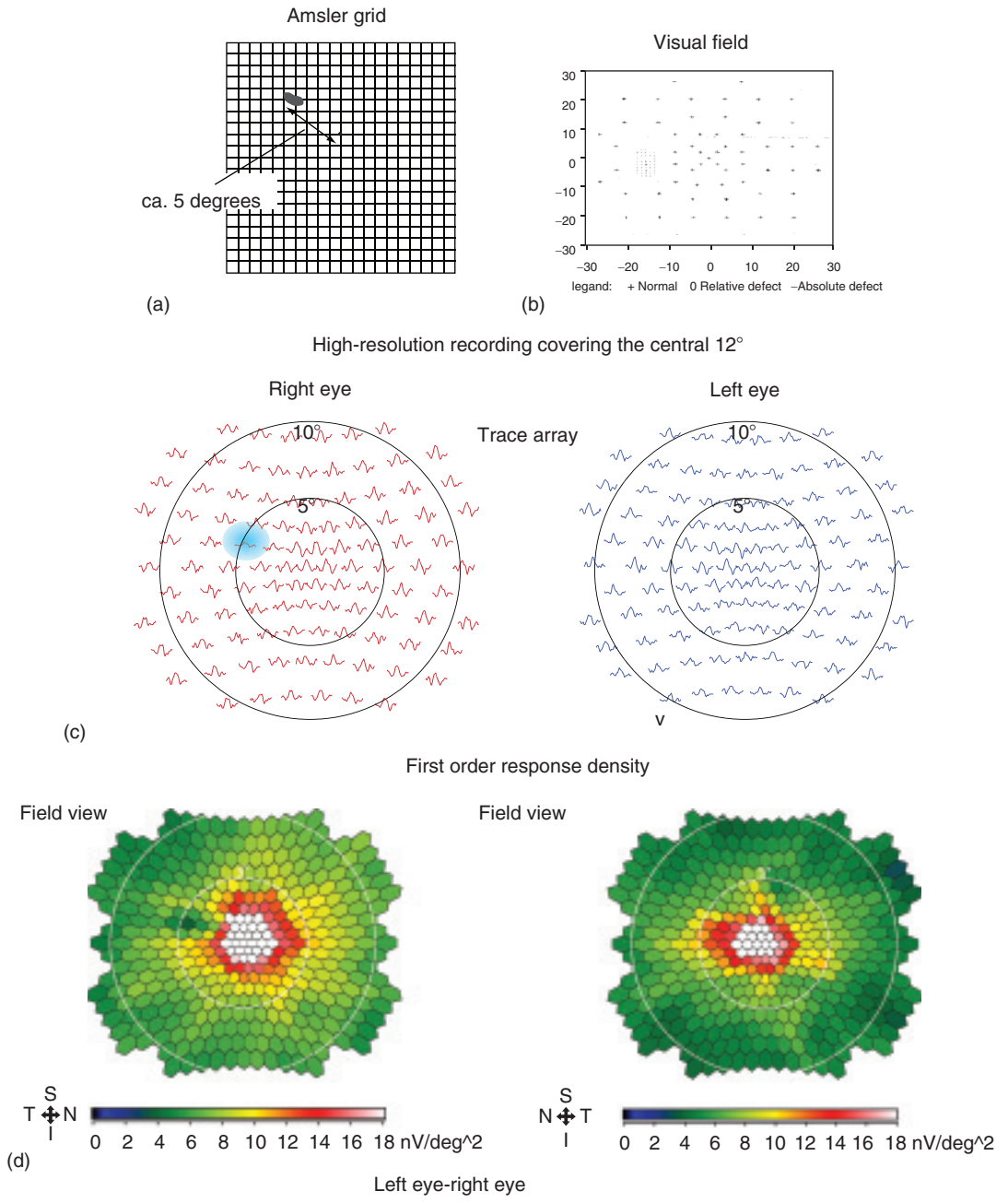

Figure 7 Patient complaining of a small scotoma not ophthalmoscopicly or in the visual field. Patient draws it in the Amsler grid. A 7-min high resolution mfERG record reveals the dysfunctional patch objectively. (a) Amsler grid, (b) visual field, (c) trace arrays, (d) response density topography.

inner retinal response contributions. However, changes in the ERG signal are rather subtle and have proven difficult to detect in early stages of disease. The ganglion cell contributions to the ERG are small and overlap with signal contributions from other retinal sources, making their isolation and quantitative estimation extremely difficult. The discovery of the optic nerve head component (ONHC) of the ERG raised hope that isolation and mapping of ganglion cell function might become possible. The ONHC is a contribution from optic nerve fibers near the optic nerve head. Its generation is schematically illustrated in **Figure 10**. The contribution of the ONHC is delayed by the amount of time it takes action potentials to travel from the stimulated retinal patch to the nerve head. It is recognized by its timing, which varies depending on the length of the nerve fibers connecting the stimulus site with the disc. Possible mechanisms for its generation are the sharp bend in the axons where they descend into the cup, the beginning of myelination near the lamina cribrosa and conductive changes in the extracellular

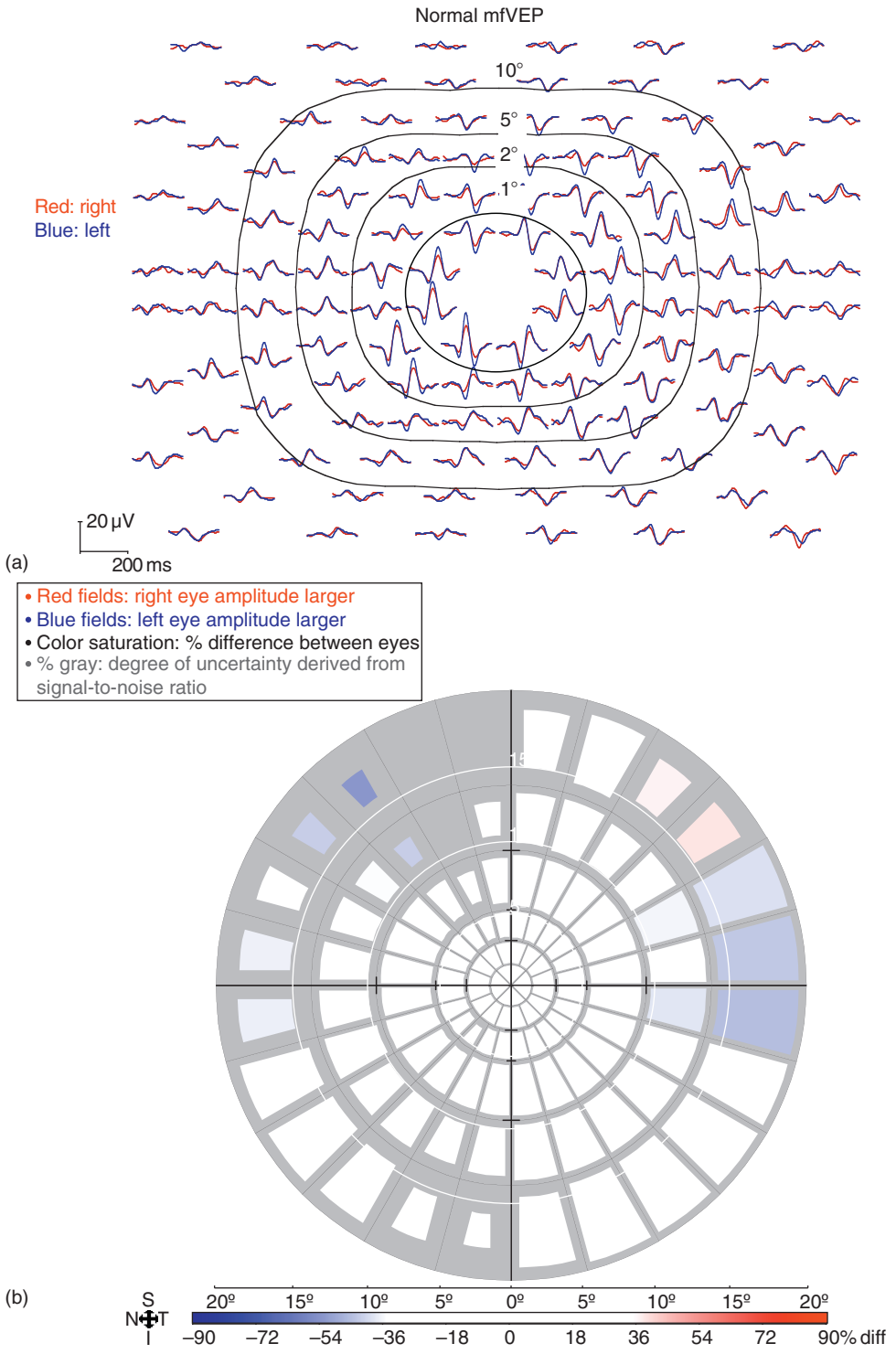

Figure 8 MfVEP of a normal subject. (a) interocular comparison of response traces: right eye red, left eye blue. The distribution of the traces is not topographic but has been arranged for best presentation of the traces in the rectangular plot area. Approximate eccentricities are indicated. (b) Pseudocolor topographic map of interocular differences.

medium. The observation that it can disappear in demyelinating disease while cortical responses are preserved, strongly points toward the transition from membrane conduction to saltatory conduction at the point where myelination begins as the main source of this signal. While mfVEP amplitudes are affected by the cortical anatomy, ONHC amplitudes directly reflect function. Their local evaluation does not require interocular response

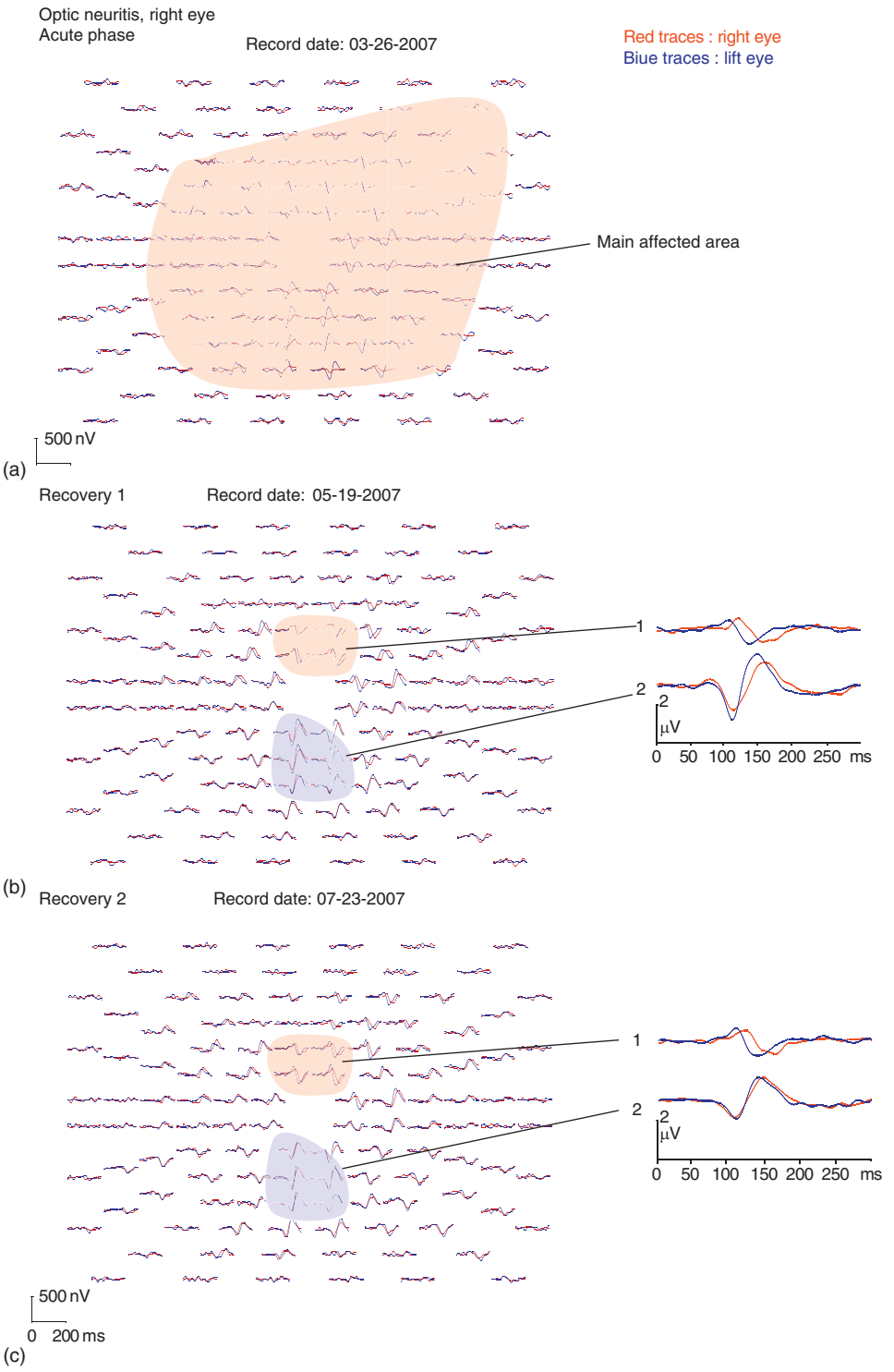

Figure 9 MfVEPs of a patient with optic neuritis. (a) during the acute phase: The red shading indicates the affected area. (b) After 2 months recovery: Amplitudes have largely recovered, but increased implicit times in the central area indicated demyelination. (c) After 4 months recovery: delays in the lower field have largely disappeared while those in the upper field remain.

comparison. In bilateral disease, the ONHC, thus, promises to be more reliable than the mf VECP.

In records collected with the commonly used mf ERG protocol, the ONHC is too small to be evaluated (**Figure10(b)** left). The traces are from a ring around the fovea starting from the area near the nerve head, proceeding through the upper field and returning through the lower field (insert on the right). The contributions

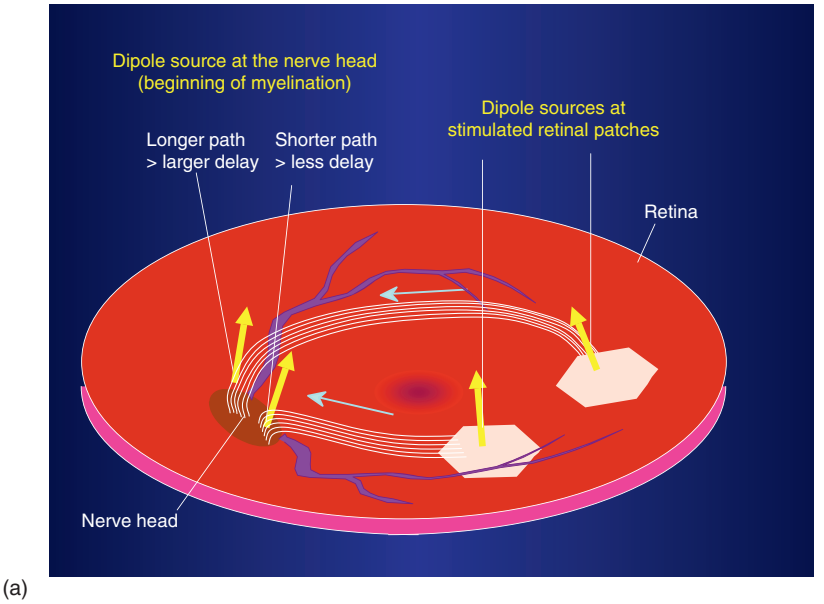

(a)

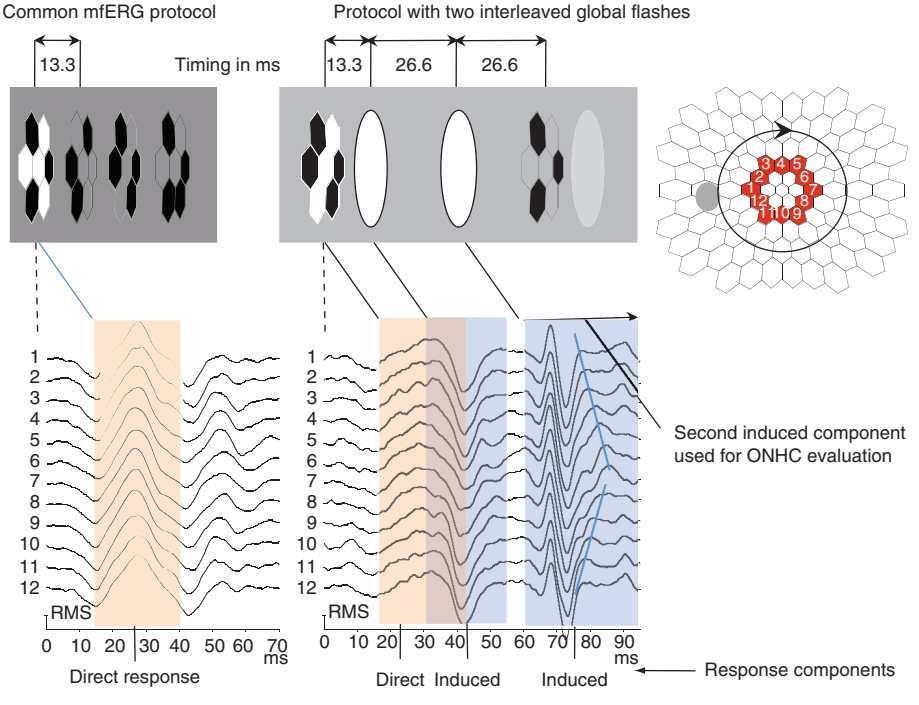

(b)

Figure 10 (a) This is a schematic illustration explaining the generation in the optic nerve head component (ONHC). Two signal sources are thought to contribute to the signal derived from the cornea, one from the stimulated retinal area and the second from the location in the nerve fibers where myelination begins. The latter is delayed relative to the retinal response by travel time of action potential from the stimulation site to the nerve head. It is recognized by this location-dependent delay. (b) Enhancement of the ONHC through the global flash paradigm. (Top) Schematic comparison of the stimulation used in the common m-sequence protocol on the left and the interleaved global flash protocol on the right. (Bottom) First-order traces derived from a normal subject: left, common protocol; and right, global flash protocol. The traces are from a ring around the fovea (insert on right) starting from the vicinity of the nerve head. The thin blue lines indicate the main feature of the ONHC contribution. The second induced component, epoch 60–90 ms, is normally used for visual evaluation.

from the ONHC should thus increase in implicit time to trace 7 and then decrease again. A stimulation protocol is now available that greatly enhances the ONHC as well as inner retinal response contributions. The protocol uses global flashes interleaved at specific intervals between the multifocal stimuli. The principle is illustrated on the right in **Figure 10(b)**. The ONHC is now readily recognized. It consists of those features in the waveforms that shift

to longer implicit times with increasing distance of the stimulus patch from the nerve head. Its main peak is indicated with a thin blue line.

The ONHC can be visually evaluated when traces on rings around the fovea are plotted in vertical columns. A plot of this kind from a normal subject is shown in **Figure 11**(**a**). Traces in each ring are plotted starting from the patch nearest the disk, proceeding through the upper field and returning through the lower field.

The delays of the ONHC relative to the retinal contributions to the ERG are known. Propagation velocity of action potentials in the unmyelinated nerve fiber layer is determined by the fiber diameter and varies little between subjects. Aligning the traces to the ONHC before applying some spatial filtering further enhances its visibility and our ability to evaluate it by visual inspection. It is now seen as a vertical ridge in the columns of **Figure 11**(**b**).

Until an algorithm for estimation of the ONHC that performs better than a visual evaluation becomes available, the ONHC is mapped and scored as follows: using the computer mouse, traces are marked pink for moderately deficient and red for severely deficient in the ONHC. The corresponding areas automatically appear pink and red in the topographic insert below together with a numeric score (see example of **Figure 12**).

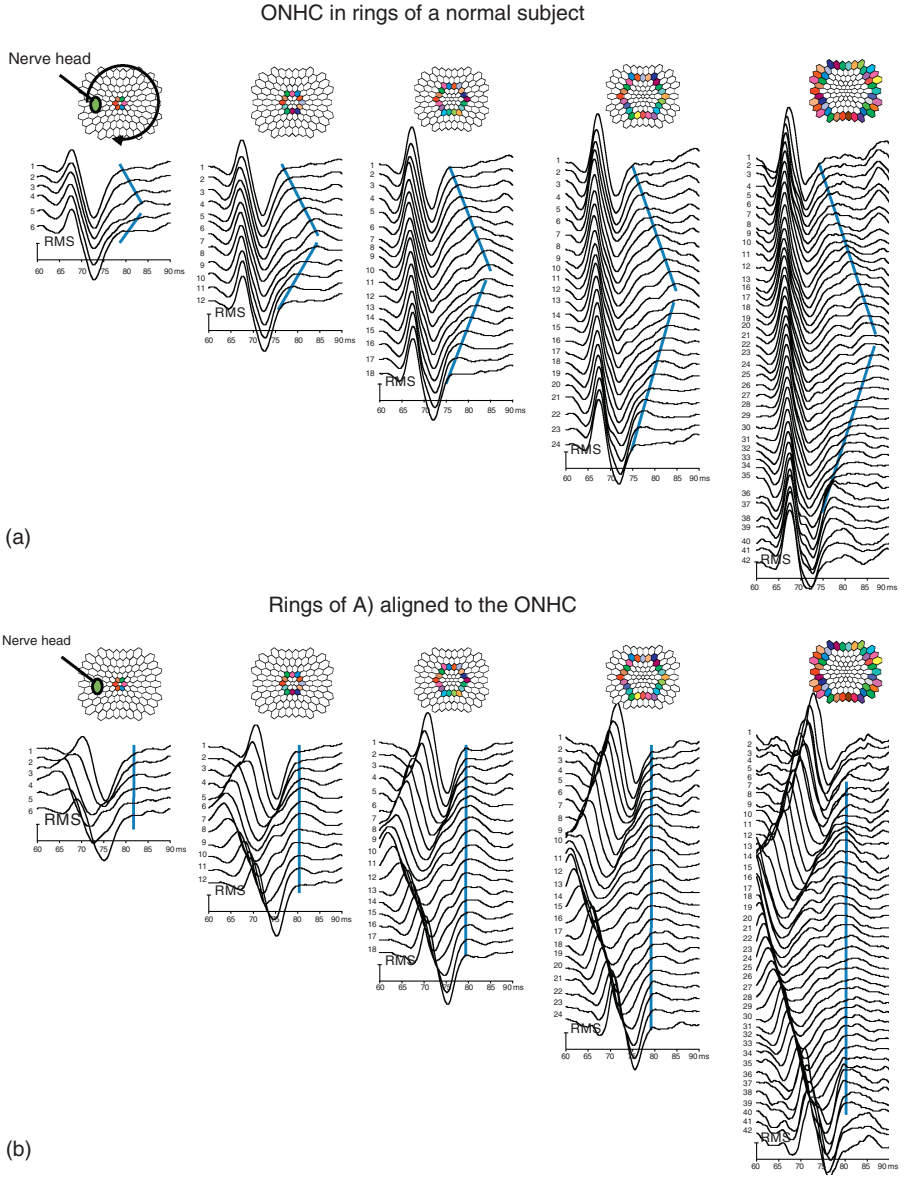

Figure 11 (a) Plots for visual evaluation of the ONHC. Traces on rings around the fovea are plotted in columns. Each ring begins on the side of the optic nerve head, proceeds through the upper field and returns through the lower field. (b) To enhance the appearance of the ONHC, the traces are aligned to ONHC implicit times.

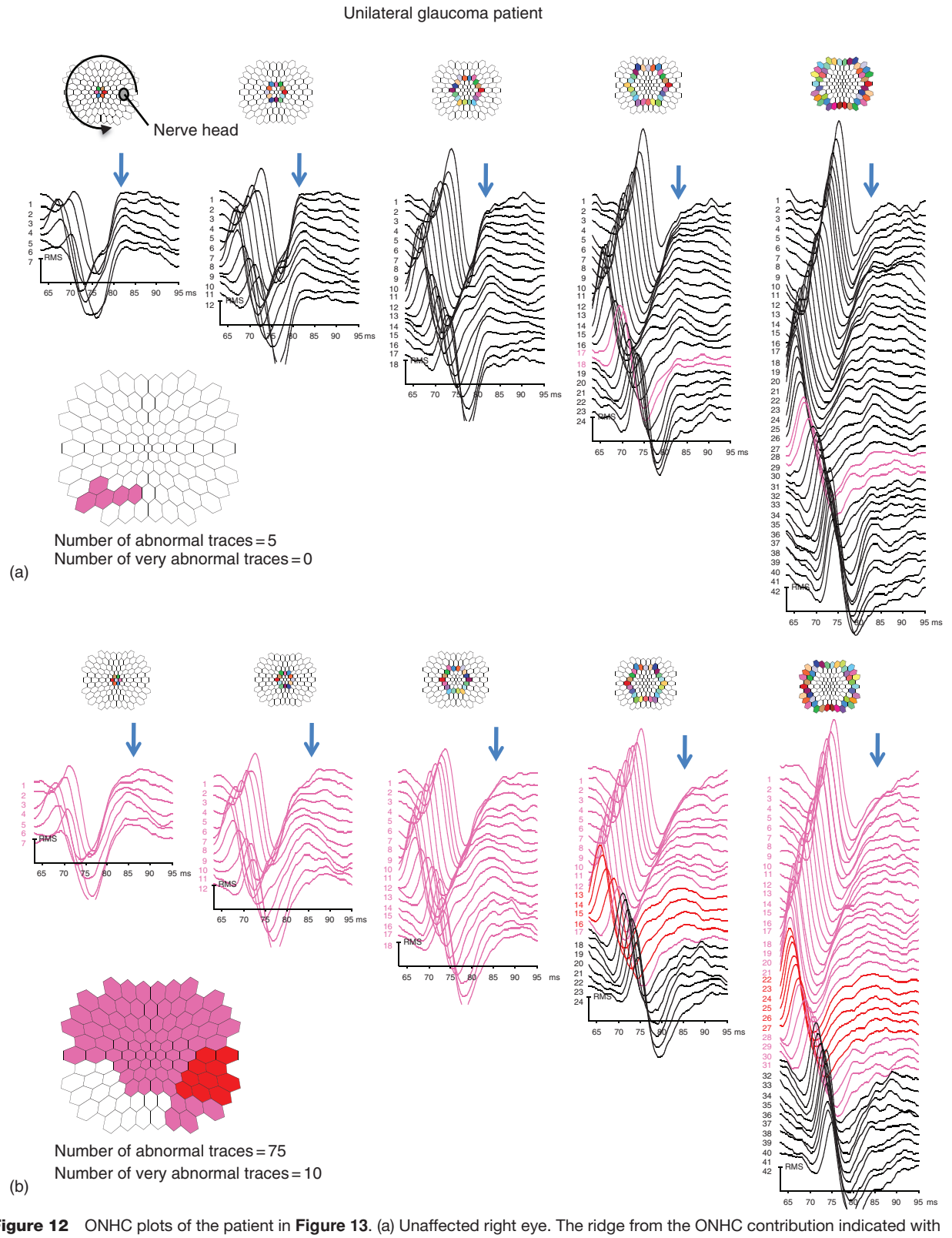

Figure 12 ONHC plots of the patient in **Figure 13**. (a) Unaffected right eye. The ridge from the ONHC contribution indicated with blue arrows is clearly visible and appears normal in most areas; (b) The ONHC ridge has largely disappeared. A residue is visible in the lower field.

Comparison of the mfVEP and the ONHC of the mf ERG in an Asymmetric Glaucoma Patient

To illustrate the performance of currently available electrophysiological function tests, a highly asymmetric glaucoma patient was selected. In **Figure 13(a)**, the mfVEP trace arrays of the two eyes are compared. **Figure 13(b)** shows an automated topographic analysis of the same data set. The color of the field indicates the eye with the larger response, red for right, and blue for left. The color saturation indicates the percent difference in response amplitude

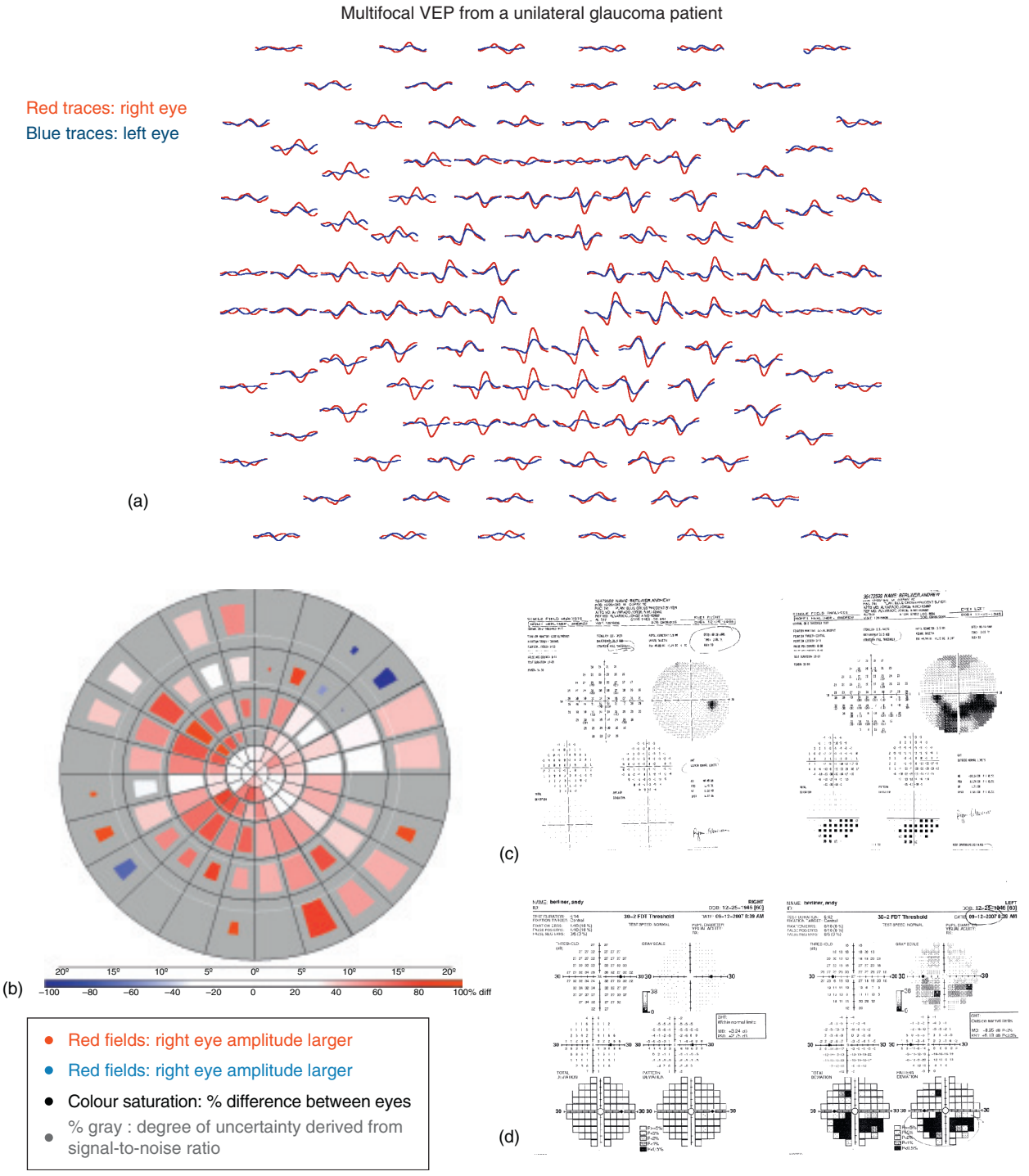

Figure 13 The mfVEP of an asymmetric glaucoma patient: (a) trace arrays of the two eyes; (b) topographic representation of interocular differences shows areas with response deficit in the left eye; (c) visual fields; and (d) perimetry using frequency-doubling technology (FDT) maps for comparison.

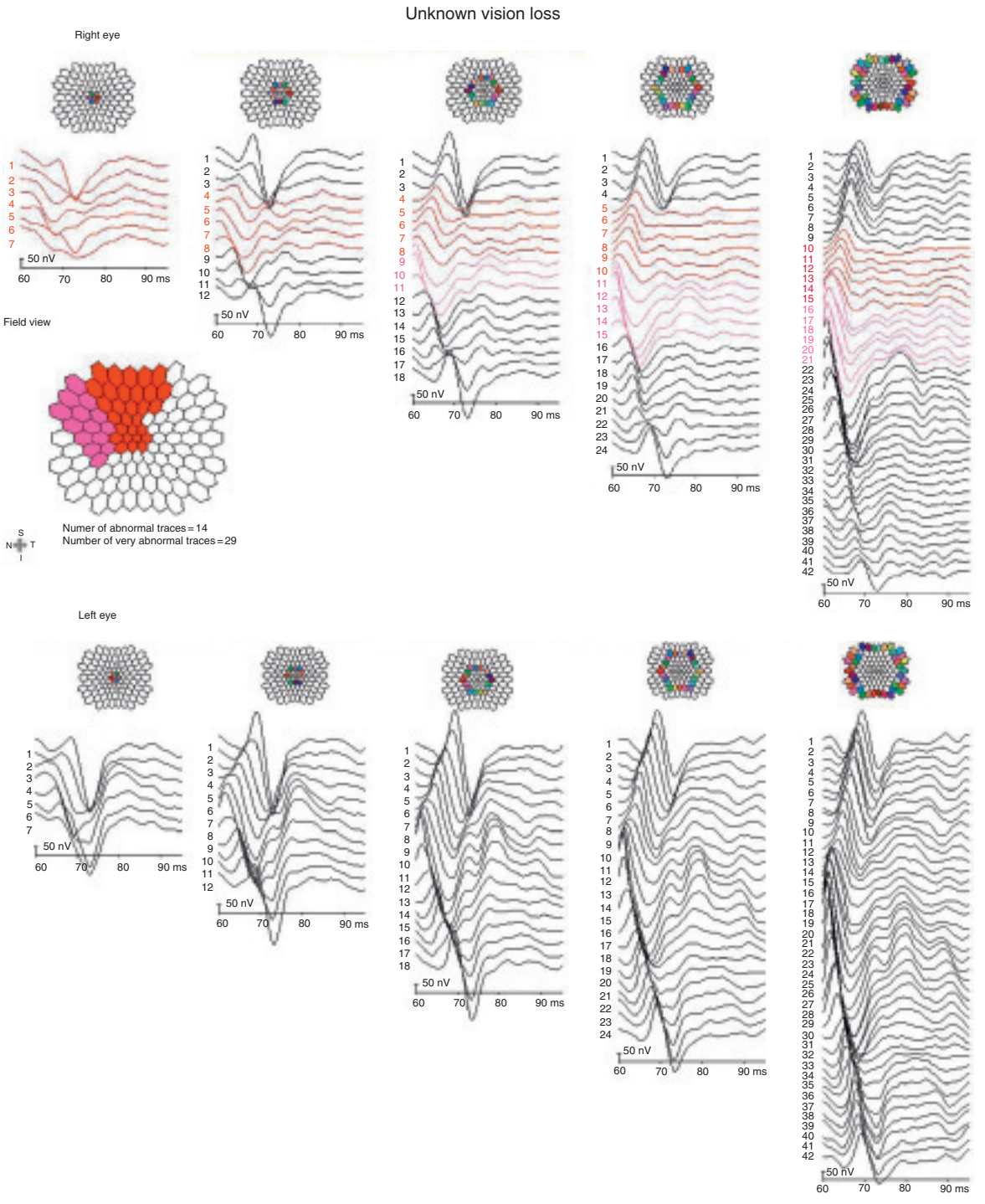

Figure 14 ONHC plots of a person with unknown vision loss. The complete disappearance of the ONHC in areas of the right eye is not consistent with the full visual field (not shown). Conclusion: The disappearance is due to loss of the transition from unmyelinated to myelinated fiber through retrolaminar demyelination rather than conduction loss.

between the eyes. The percentage of gray in each field represents the uncertainty in the estimate based on the signal-to-noise ratio in the record. The numeric version of the plot is not shown here. The inserts (c) and (d) show the visual field and the field mapped with the frequency-doubling technique (FDT) for comparison. **Figure 12(a)** and **12(b)** show the ONHC analysis of the mfERG for the two eyes of the same subject. Traces judged deficient in the ONHC are marked pink or red by the operator depending on the degree of abnormality. The corresponding stimulus areas are marked in the same color in the inset below.

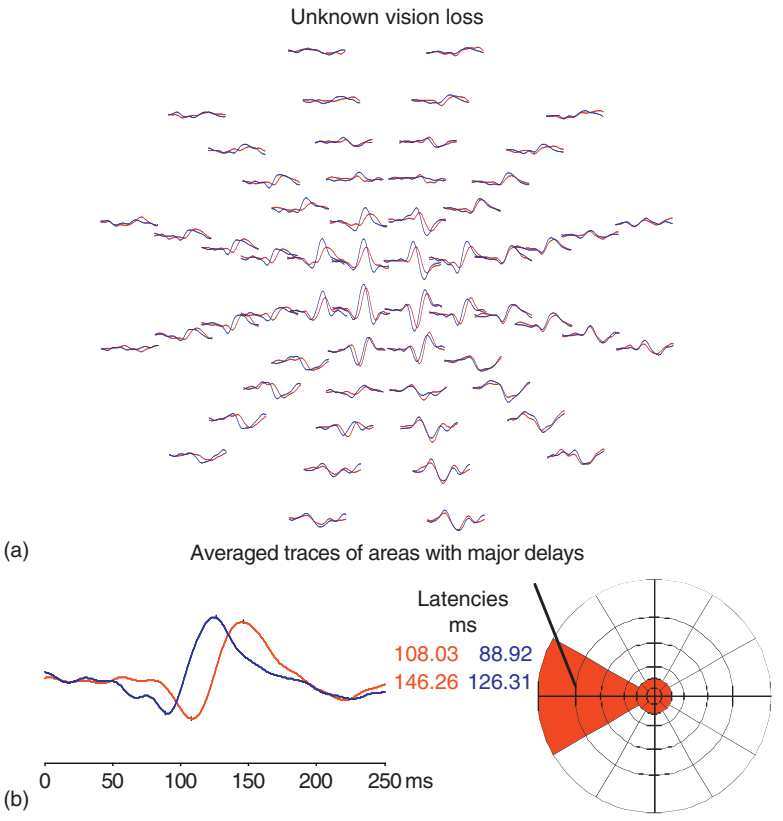

Figure 15 The conclusion from **Figure 14** is confirmed with an mfVEP. In the right eye, we find areas with substantial delays.

Both, the mfVECP and the ONHC data show more extensive losses than the two psychophysical function tests. In such highly asymmetric cases, the mfVECP can be a very sensitive test. It becomes more problematic when both eyes are affected. The ONHC, on the other hand, does not require interocular comparison.

Patient with Unknown Vision Loss

A 53-year-old male patient noticed blurring in his right eye. His visual acuity was V/A 20/30 on the right and 20/20 on the left. Visual fields were normal in both eyes. The common first-order response is somewhat lower in the right eye, but its topographic distribution is within normal range (not shown). The ONHC, on the other hand, is highly abnormal in the right eye, particularly in the center and in some portions of the upper field and completely absent in some areas (**Figure (14)**). The left eye is within normal range. The gross abnormalities in the ONHC are not consistent with the normal visual fields of the patient (not shown). This finding could, therefore, not be attributed to loss of nerve conduction. It could, however be explained by retrolaminar demyelination eliminating the source of the ONHC. This reasoning led to the mfVEP records shown in **Figure 15**. In the right eye, the responses are indeed substantially delayed in the areas with an abnormal ONHC confirming local demyelination. This case is interesting as electrophysiology led to the diagnosis of a patient not suspected of demyelinating disease.

Note that the ONHC is abnormal in some cases of optic neuritis even when substantial cortical delays are observed but not in others. In the above example, there are large cortical delays in areas where the ONHC is preserved. In the case of acute optic neuritis (**Figure 9**), the ONHC was judged within normal range in both eyes. In combination, the three tests (common mfERG, ONHC, and mfVEP protocols) allow us often to localize a dysfunction along the visual pathway.

Summary and Conclusion

Multifocal electrophysiology is not a single tool, but rather a collection of tools. Stimulation and analysis protocols can be optimized for specific clinical applications such as diabetes, AMD, optic neuropathies, etc. Much can still be done to shorten the tests and improve their efficiency. The protocols can be semiautomated to make clinical testing easy. However, the tools have to be paired with the expertise necessary to select the proper tool for each case and interpret the data.

There is a great deal of information contained in multifocal records that is only partially understood and still largely unexploited. Combining tests of function and structure promises to advance the understanding of both types of data and the pathogenesis of diseases. A case in point is the example of x-linked retinoschisis shown in **Figure 6**. The availability of OCT data on the different areas of the retina might have greatly helped our understanding of the connection between function and stricture in this and other similar cases.

Acknowledgment

The studies on which this article is based have been supported in part by NIH grant EY06961.

See also: Adaptive Optics; Optical Coherence Tomography; Primary Photoreceptor Degenerations: Retinitis Pigmentosa; Primary Photoreceptor Degenerations: Terminology; Secondary Photoreceptor Degenerations: Age-Related Macular Degeneration.

Further Reading

Hood, D. C. (2000). Assessing retinal function with the multifocal ERG technique. *Progress in Retinal and Eye Research* 19: 607–646.

Miyake, Y. (2008). *Electrodiagnosis of Retinal Diseases*. Tokyo: Springer.

Sutter, E. E. (2001). Imaging visual function with the multifocal m-sequence technique. *Vision Research* 41: 1241–1255.

Sutter, E. E. (1992). A deterministic approach to nonlinear systems analysis. In: Pinter, R. B. and Nabet, B. (eds.) *Nonlinear Vision*, pp. 171–220. Cleveland, OH: CRC Press.